Chapter 8

The Birth

The moment of star birth is here *defined* as the instant at which a final static core has come into existence. Its mass is tiny in comparison to the final mass it will achieve. It is merely the central object, the baby, which will accrue material from the nurturing core. The moment probably corresponds to the instant at which there is no going back; the formation of a stellar system or star is inevitable. If the baby is not adequately fed, however, it may have to settle to be a brown dwarf. Or, if essentially starved, a lonely planet.

In this chapter, we describe the youngest protostellar stages and discuss the processes and problems which nature presents. First, however, we must determine if we really have observed a birth. As always, we are led by the observations and need to sort out the observational signatures which reveal how long a protostar has been alive. The interpretation remains challenging and problematic since we cannot directly observe the processes. In addition, evolutionary models don't quite succeed.

We continue our stellar biography from the proposed moment of birth. In so doing, we reverse the historical path of discovery which led from the adolescent young stars which were optically visible (Class III) back in evolution to the protostars (Class I). The holy grail was later uncovered in what was then labelled as the Class 0 protostar: a core which does not contain a Class I protostar, yet in which a collapse has brought into being a central object. To present our epic journey from cloud to star, we introduce the objects in the reverse order to their discovery.

The signatures and evolution are significantly different for stars which end up like our Sun (low-mass stars) and hot OB stars (high-mass stars). We concentrate on the birth of low mass stars here and the formation of high mass stars in §10.10.

If in the Class 0 protostar we have truly uncovered the defining moment,

then we have unified our evolutionary studies. One set of astronomers were attempting to follow the evolution of molecular clouds, discovering regions of increasing compactness. Other groups were tracing back the evolutionary tracks of young stars. Now, we could link the two together and present a continuous evolution all the way through. Things are never quite that simple of course. The new complexity is that the evolution is rapid: clouds and young stars evolve simultaneously in the same region. They also interact, influencing or even regulating each other's evolution. Finally, it must be questioned whether the search is really over or whether there are objects and stages still to be discovered.

8.1 Commencement of Life

The critical moment is called *Age Zero* by some. It is actually the point at which a protostar rather than a star is brought to life. The protostar is contained within a protostellar core, distinguished from the 'starless cores' (actually 'protostar-less-cores') described in the previous chapter. One could define a star's life to begin at other critical moments, raising similar controversies to that surrounding the beginning of human life. We could instead choose the core itself as the baby, or wait until hydrogen nuclear burning has begun. By analogy, however, cores are commonly treated like eggs while nuclear burning represents the approach towards adulthood.

Age Zero should help define a unique clock for each star. We take it to correspond to the moment when a gaseous sphere is thermally enclosed for the first time. Enclosure is reached in the state where photons cannot directly escape from a sphere but are radiated from a photosphere. There is a bottleneck of photons within the photosphere: the energy reservoir inside cannot be efficiently emptied. This concept of birth corresponds to Stage 3 of the approach to birth discussed in §6.6, at the end of the first collapse. Nevertheless, this event is only about 2,000 years before the final collapse of Stage 7.

A rather subjective date of birth is also associated with the instant at which a young star is exposed to us in the optical or visible part of the spectrum. After this, the object can be treated with the traditional tools developed for stellar evolution. That means we can find its temperature and luminosity and so, from then on until its death, predict its evolution as a track on the standard Luminosity-Temperature diagram (Fig. 9.2) or 'Hertzsprung-Russell' diagram (Fig. 9.2), as described below. A 'birthline'

is then expected. This line is the predicted locus of points on the diagram which divides an empty region (obscured protostars) from optically-detectable young stars of all possible masses.

8.2 Identifying and Classifying Protostars

How can we determine the evolutionary status of a star that we can't even see? The status of a star in classical astronomy is determined by locating it on a Hertzsprung-Russell diagram (Fig. 9.2). This requires measurement of a star's luminosity and colour. The luminosity is determined from its observed flux and distance. The colour is closely related to the wavelength at which the emission peaks which is determined by the effective surface temperature if it is a blackbody. The surface temperature can also be deduced by measuring atomic spectral lines and applying some atomic physics since many lines are sensitive indicators of the temperature. Visible stars are therefore also classified in terms of luminosity class and spectral type.

The trouble is that young stars and protostars are not classical stars, as is clear from Fig. 8.1. At optical wavelengths, the youngest stars are rendered invisible. They are often not blackbodies and the spectral type is often absent or ambiguous. For the deeply embedded stars discussed in this chapter we only see light which has been processed by the enveloping core out of which they grow. Gas and dust absorb the protostar's radiation and re-radiate it at much longer wavelengths. Even at infrared wavelengths, such protostars can be hard to detect. As a further complication, the escaping radiation from the circumstellar material usually arises from a wide range of distances from the central source, generating an extended continuous spectrum which does not resemble a blackbody.

Nevertheless, we can still determine the total luminosity escaping from the envelope given enough observations spread over the wide continuum. Such broad-band photometric observations are crucial for the understanding of protostars. The resultant radiated power is called the bolometric luminosity.

We also need an appropriate substitute for the optical colour. Two possible substitutes have been seriously considered. The established method was originally proposed by Charles Lada and Bruce Wilking in 1984. It involves the properties of the *spectral energy distribution*, or SED, the distribution of radiated power with wavelength. Rather than following the radiated power per unit wavelength, S_λ, we study the distribution of $\lambda \times S_\lambda$.

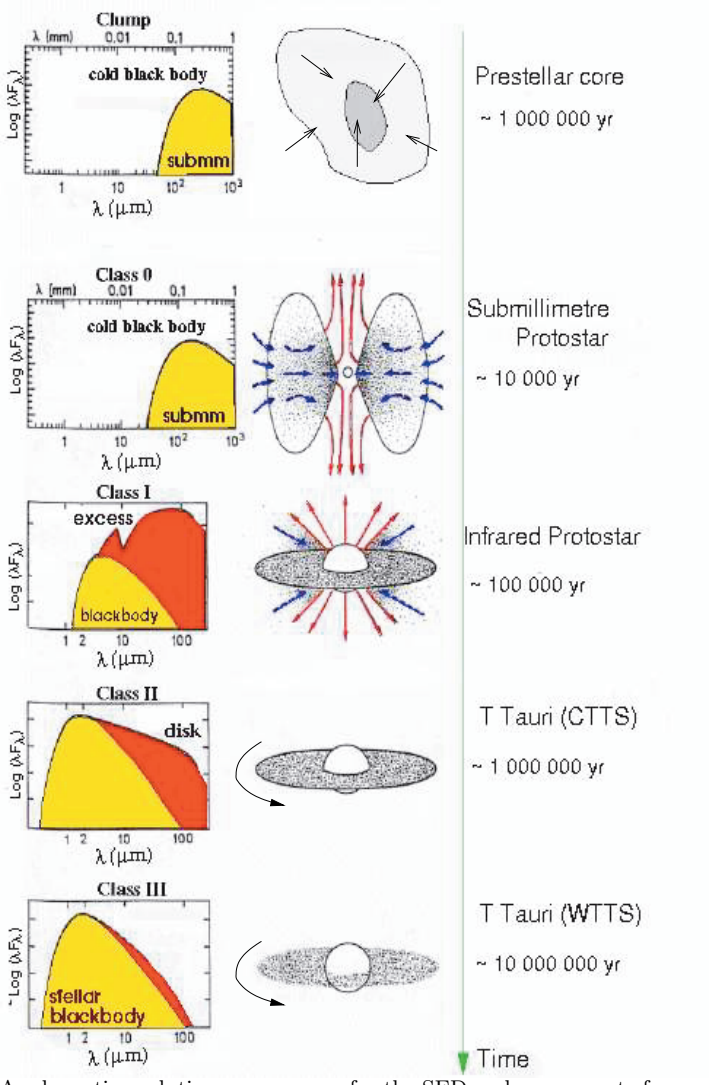

Fig. 8.1 A schematic evolutionary sequence for the SED and components from embedded clumps to naked young stars. (Credit: adapted from C. Lada, P. André, M. Barsony, D. Ward-Thompson.)

More precisely, we calculate a property of the SED measured over a narrow range in wavelengths: the infrared SEDs. The earliest protostars should be still surrounded by massive infalling envelopes which radiate copiously in the far-infrared. In contrast, more advanced stages, where the envelope has

been incorporated into the star or dispersed, should radiate strongly in the near-infrared and optical. Therefore, the slope of the SED in the infrared ought to provide an empirical evolutionary sequence.

Four broad classes of young stellar object are usefully defined. These are designated as Class 0, I, II and III and illustrated in Fig. 8.1. In this chapter, we restrict our attention to the Class 0 and Class I sources which peak in the submillimetre and far-infrared portions of the spectrum, respectively. Whereas S_λ gives the luminosity within each unit wavelength interval, $\lambda \times S_\lambda$ is a quantity which emphasizes the dominating spectral region. To obtain a spectral index which describes the form of the power-law function, we take the logarithm and fit a straight line. The slope of this line α_λ across the wavelength range 2–20 μm defines an infrared spectral index:

$$\alpha_\lambda = \frac{d(\log \lambda S_\lambda)}{d(\log \lambda)}. \tag{8.1}$$

Often, it is more useful to employ the frequency as the variable:

$$\alpha_\nu = \frac{d(\log \nu S_\nu)}{d(\log \nu)}, \tag{8.2}$$

in which case $\alpha_\nu = -\alpha_\lambda$.

Class 0 and I are then defined as possessing infrared SEDs that rise with increasing wavelength. That is, the spectral index is positive ($\alpha_\lambda > 0$). They are sources thus identified as young protostars, deriving most of their luminosity from accretion, embedded in a massive envelope. More precisely, we will use the terms Class 0 and Class I *sources* to describe the types of cores which contains the Class 0 and Class I *protostar* in their interior. respectively.

To divide Class 0 from Class I protostars, we require a further empirical border based on how we expect a protostar to evolve. We have seen that most of the luminosity of a low-mass core is emitted at infrared wavelengths because higher energy radiation from the central protostar is reprocessed by dust grains in the envelope. These heated grains also emit detectable radiation at submillimetre wavelengths. This cold dust emission samples the entire mass contained within the extended envelope because the envelope is optically thin at such long wavelengths. Class 0 sources are defined to be cores which possess a central protostar, but which have $L_{smm}/L_{bol} > 0.005$, where L_{smm} is the luminosity at wavelengths exceeding 350μm. Clearly, if we presume that the quantity L_{smm}/L_{bol} will only decrease with time, as

the cool envelope fades, then this definition should pick out the youngest protostars.

The second colour substitute is the bolometric temperature. This entails numerous measurements over a wide range of wavelengths with a range of telescopes, measurements which are now becoming increasingly achievable. When accomplished, the bolometric temperature may be a guide to the phase in the growth of the protostar, increasing with age. For a blackbody, the wavelength range within which the quantity $\lambda \times S_\lambda$ peaks automatically yields the bolometric temperature, as defined by Eq. 6.7.

Fortunately, so far there has been no serious contradiction between the two systems. Quite sharp divisions in the bolometric temperature correspond to the class divisions. Class 0 corresponds to protostars with $T_{bol} < 70\,\mathrm{K}$ and Class 1 to $70\,\mathrm{K} < T_{bol} < 650\,\mathrm{K}$. To see how closely these classes correspond to a physical classification, we require an interpretation. This, of course, requires a model. However, even if we assume a systematic development, the bolometric temperature is more likely to be controlled by the luminosity rather than the age. Therefore, until we have more data, interpretations remain open.

8.3 Observations of Protostellar Cores

In the past, only single bolometers were available to detect the emission from the cores. Now, high sensitivity submillimetre bolometric arrays, such as SCUBA, allow us to map the dust emission from the envelopes. The resulting picture is still being pieced together.

We are finding that cores which have successfully given birth appear generally very different from starless cores. They reveal their new status by taking a more compact shape. Starless cores tend to have a flat density profile at small radii and are bounded or sharp-edged at some outer radius, thus resembling finite-sized Bonnor-Ebert spheres. In contrast, the density in protostellar cores is more centrally peaked with a density profile corresponding closer to the form $\rho \propto R^{-2}$.

Furthermore, the velocity structure is distinctive. Infall signatures are much more obvious and they exhibit broader lines attributed to substantial turbulence. The origin of this turbulence is thought to be the protostar itself which feeds kinetic energy back into the core not only through the release of gravitational energy in the form of radiation, but also through jets in the form of kinetic energy (see §9.8). Typical values for the width

of NH_3 lines are 0.4 km s^{-1} in protostellar cores as opposed to 0.3 km s^{-1} in starless cores. Similarly, the average width of $C^{18}O$ lines are 0.6 km s^{-1} in protostellar cores as opposed to 0.5 km s^{-1} in starless cores.

Although the cores are gravitationally bound, they are not usually observed in isolation. What spatial scales of core clustering are set during star formation? How does a clump fragment into star-forming cores as it contracts? To answer these questions we have begun to trace the number, relative position and extent of cores. Molecules with large dipole moments such as CS, H_2CO (formaldehyde) and HCN (hydrogen cyanide) are good tracers of the density because of the large volume density required for thermal collisional excitation. Symmetric top molecules such as methyl cyanide (CH_3CN) are good tracers of temperature.

Three morphological types of cores are distinguished observationally: independent envelope, common envelope and common disk systems. The independent envelopes are separated by over 6,000 AU. Common envelope systems consist of one large-scale core which splits into multiple components on the scale 150–3,000 AU. Common disk systems lie within the same disk-like structure on scales of $\sim$ 100 AU. These structures must be related to the nature of the resulting stellar system. This requires an understanding of the fragmentation processes which we examine in §12.5. Here, we focus on the individual cores and the primary protostar growing within.

8.3.1 *Class 0 protostars: the observations*

Class 0 sources are surrounded by large amounts of circumstellar material. They are so highly enshrouded that their SEDs peak longward of 100 μm and their near-infrared emission is very faint. Most are not even detected shortward of 20 μm. One example of a Class 0 SED is displayed in Fig. 6.1. The spectral widths are quite similar to those of single temperature blackbody functions with temperatures in the range 20–70 K, warmer than starless cores.

All Class 0 sources are associated with molecular bipolar outflows. The outflows are high-powered and well-collimated. These will be described in §9.8. Observationally, they are signposts for otherwise hidden protostars. Physically, they may prove to be a necessary consequence of a process essential for the final collapse: channels for removing excess angular momentum.

8.3.2 *Class I protostars: the observations*

Class I SEDs are broader than predicted by single blackbodies and peak in the far-infrared. Nevertheless, we can associate bolometric temperatures through Eq. 6.7. We find that the range $70\,\mathrm{K} < T_{bol} < 650\,\mathrm{K}$ covers Class I objects. There is a huge 'infrared excess' and they often exhibit a sharp absorption feature at 10μm due to silicate dust. Hence, a large amount of warm circumstellar dust generates the infrared properties.

Although obscured from view in the optical, atomic emission lines are observed in the infrared. Apart from this, the infrared is virtually featureless and heavily veiled (i.e. the continuum dominates at all wavelengths). A significant fraction of the near-infrared emission is scattered light, detected as a small near-infrared reflection nebula.

Class I sources are also often associated with molecular bipolar outflows. They are typically less energetic than the Class 0 outflows but the vast majority of detected molecular outflows are driven from Class 1 sources.

It is not clear how the luminosity evolves. Class I protostars are not significantly less luminous than Class 0 protostars. The luminosity range is $\sim$0.5–50 $\mathrm{L}_\odot$. They are however, more luminous than the older Class II sources in the ρ Ophiuchus region but not in the Taurus region.

How can we be sure that these sources are protostars and not some other type of star which happen to be embedded? There are several pieces of evidence:

- They are located within star-forming clouds.
- Modelling in terms of a rotating and infalling cloud core is able to reproduce the features of the SEDs.
- Inferred mass infall rates are of order 10^{-5} $\mathrm{M}_\odot$ yr^{-1} which implies that a solar mass star could form in 100,000 years. This is consistent with their statistically determined lifetime.
- The infrared excess indicates that there is plenty of heated dust close to the source. This dust would be blown away by radiation pressure and would not survive in a steady state in this region. Therefore, a dynamically infalling envelope is suggested.
- Direct kinematic evidence for infall has now been observed in a number of Class 0 protostars. The signature is an asymmetry in the line profiles in which the red-shifted portion of an optically thick emission line is depressed relative to the corresponding blue-shifted portion. In fact, the first example of this signature was that of IRAS 16293-2422, observed in transitions of CS.

8.4 Theory of Accretion onto Core

Figure 8.1 shows schematic pictures of the main components of protostellar systems: the central protostar, the circumstellar disk, and the surrounding envelope. The observed Classes are interpreted in terms of these three physical components as follows.

The central protostar is classified as a Class 0 protostar as long as $L_{smm}/L_{bol} > 0.005$. This was originally meant to correspond to the case where more than half of the total mass of the system is still in the infalling envelope. After half of the mass of the envelope has fallen in, the source is referred to as a Class I protostar. This, however, depends on the chosen model for the mass–luminosity relationship.

Once almost all of the envelope has been accreted (or otherwise dissipated), the source is referred to as a Class II source or Classical T Tauri star (CTTS). At this stage, there is still a substantial circumstellar disk, which may go on to form planets.

Finally, when the inner part of the disk has dispersed, it is known as a Class III source or a weak-line T Tauri star (WTTS).

The processes by which material moves between the components, from the outer envelope to the central protostar, are still under debate. Theories differ primarily in their predictions of the density, $\rho(r,t)$, and velocity, $v(r,t)$, as a function of radius, r, and time, t. Cores are, however, as a rule not uniform or spherical and the observed quantities are angle-averaged. The three broad categories of theory are founded on:

(1) the loss of gravitational stability and collapse of a static core,
(2) the triggered compression and collapse of a static core and
(3) the gravitational collapse of a fragment produced dynamically through turbulence.

In other words, the interpretation of protostellar cores depends on the chosen *initial conditions*. Once we know $\rho(r,t)$ and $v(r,t)$, the predicted evolutions can be compared through the mass accretion rates given by

$$\dot{M}(r,t) = -4\pi r^2 \rho(r,t) v(r,t). \tag{8.3}$$

We can calculate how the bolometric luminosity evolves from the energy released during the accretion. Protostellar sources begin by being gravitationally powered; the nuclear power from the protostar is low. We assume that the radiation escapes on a timescale that is short in comparison to the dynamical timescale and that the energy leaks out (or is stored) in no other form. Then, the gravitational energy released per unit accreted mass

is approximately GM_*/R_* for a protostar which has reached a mass M_* and radial size R_*. This is because most of the energy is liberated abruptly at an accretion shock near the protostellar surface. The accretion shock may take the forms of a spherical shock and an equatorial shock, according to how the material approaches. That is, we simply take the potential energy from infinity to the protostar's surface. This energy multiplied by the rate at which mass accretes $\dot{M}(R_*, t)$ onto the surface yields the total energy released, called the accretion luminosity:

$$L_{bol}(t) = \frac{G\dot{M}M_*}{R_*}. \tag{8.4}$$

This formula will be more accurate, the more the gravitational energy is released from close to the protostellar radius and the closer the accretion is to being uniform. However, some gravitational energy is obviously released during the initial collapse phase before protostar formation. This energy is transferred into the gas via compressional heating and could be detected in the future.

To determine L_{bol} we also need to know how the protostar is growing. While $M_*(t)$ corresponds to $\dot{M}$ integrated from Age Zero up to time t, the radius $R_*(t)$ requires some knowledge of the density in the protostellar interior. Moreover, there are more assumptions needed. For example, some of the mass may be diverted into a secondary protostar or smaller objects, and some may be diverted into an outflowing wind or jets. Despite these unknowns, astronomers are irrepressible and we expect to eventually take these factors into account.

8.5 Accretion Rates from Static Initial States

Initial conditions of uniform density and zero velocity were examined by Larson and Penston in 1969. This classical model encounters problems due to its prediction of supersonic infall velocities that are not observed in regions of low-mass star formation. Perhaps a more consistent static initial condition is a Bonnor-Ebert sphere in which a uniform density is approached only in a central region. Computationally, an equilibrium sphere is set up and then perturbed. Hydrodynamic calculations of the collapse subsequent to protostar formation show that the density approaches a R^{-2} radial distribution at small radii. The accretion rate in this case is not constant in time but rises sharply and then falls gradually.

There are just two fundamental parameters determining accretion rates: the speed of sound, c_s, and the gravitational constant, G. This is, in essence, because thermal pressure gradients balance gravity ($M \sim \beta c_s^2 R/G$) and the timescale is $t \sim R/c_s$ Together, they yield a mass rate of

$$\dot{M} \sim \beta \frac{c_s^3}{G}, \tag{8.5}$$

where β is a constant of order unity.

In 1977, Shu proposed a scenario where infall begins from the inside, i.e., an inside-out collapse. The initial density configuration is a singular isothermal sphere with a $\rho(R) \propto R^{-2}$ power law. The collapse region begins at the centre and is bounded by the front of an expansion wave which propagates outward at the sound speed, c_s. Outside this wave, the cloud core is at rest and retains its initial density structure. Inside, the material is nearly in free-fall and the density asymptotically approaches the form $\rho(R) \propto R^{-1.5}$ and the velocity distribution is $v(R) \propto R^{-0.5}$. This free-fall state implies that the rate at which mass accretes onto the protostar is a constant. The actual value of β is in the range 0.97–1.5, yielding

$$\dot{M} = 1.6 - 2.4 \times 10^{-6} \left(\frac{c_s}{0.19 \text{ km s}^{-1}} \right)^3 \text{M}_\odot \text{ yr}^{-1}, \tag{8.6}$$

for all radii and, in principle, until the envelope is exhausted. This model has been widely explored, partly because it is based on a relatively simple, semi-analytical similarity solution, allowing rotation and magnetic fields to be treated as perturbations.

In comparison, the accretion from perturbed Bonnor-Ebert spheres begins with a sharp rise, peaking at various values but with a maximum achievable accretion rate of $\sim 47\, c_s^3/G$. High rates are not maintained for longer than a few tenths of a free-fall timescale and the accretion rate falls gradually, eventually falling below that of Eq. 8.6.

Another type of collapse is initiated by a strong external trigger rather than a small perturbation. If a static core is triggered by an interstellar shock wave, a high rate of accretion can be produced through the strong shock compression. There is indeed plenty of evidence for triggering, as now listed:

- Cometary clouds take on a wind-blown appearance: a sharp arc-shaped edge or surface and an extended tail. Many contain deeply embedded protostars.

- Molecular clouds face a potential source of a supernova shock or wind from a massive star (e.g. the Orion clouds). Triggered star formation by a distant supernova is also suggested in the Upper Sco association and the ρ Ophiuchus cloud. The star formation in NGC 2265 IRS in the Cone nebula also shows the signs of triggering by a stellar wind from a B2 star.
- Bright-rimmed globules are identified by a curved ionisation front (bright rim) on one side of their surface. They are exposed to strong UV radiation from a nearby OB star. The physical conditions of such clouds are consistent with models of a radiation-driven implosion.
- Groups of young stars sometimes appear to be ordered in space in a sequence of increasing age.
- The Solar system may have also originated from a triggering event. The evidence is derived from studies of meteorites which contain short-lived isotopes. The isotopic abundances in chondrules, in particular short-lived parent radionuclides, could have been obtained from stellar ejecta originating from a supernova and/or an asymptotic giant branch star.

Triggering has been simulated by following the evolution of a Bonnor-Ebert sphere after it has been subjected to an increase in the external pressure. The simulations demonstrate that the main features of the density and velocity field of pre-stellar cores and protostars are reproducible, and that the accretion rate is high in the earlier accretion phase. The predicted velocity field is very different from that of the standard model since the collapse begins from the outside. In many other respects, the triggering model resembles the turbulent cloud model, that we now discuss, since both are based on the impulsive compression of dense regions. For triggering, an equilibrium cloud must first be present.

Other models exist that adopt different initial conditions with various predictions for the density and velocity distributions. Therefore, observational determinations of both of these distributions can help us to discern the physical processes governing the formation of low-mass stars.

8.6 Protostellar Accretion from Turbulent Clouds

Analytical models for turbulence have proven extremely difficult to establish. We therefore rely upon numerical simulations which include as much

of the physics as we can manage. Practically all simulations have treated the formation of cores and the evolution within cores as distinct problems.

To date, the 'clumps' found in hydrodynamic simulations of isothermal turbulence possess properties that resemble the observations of cores. While encouraging, the picture is still being assembled. A quasi-equilibrium clump mass spectrum is produced in the simulations with a power-law distribution $dN/d(\log M) \propto M^{-0.5}$. This is consistent with the observed mass distributions of clumps (see Eq. 6.8). The dense, Jeans-unstable gas clumps collapse and form protostellar cores that evolve through competitive accretion and many-body interactions with other cores. In contrast to the clumps, the core mass spectrum is best described by a *log-normal* distribution that peaks approximately at the average Jeans mass of the system. A log-normal is a Gaussian distribution as given by Eq. 3.1 with the variable v replaced by $\log M$. It is the distribution often encountered when many different mechanisms are influencing an outcome. However, the observed distributions of cores differ in that they possess a power-law tail of high mass cores (e.g. cores-rhooph) which is also imprinted in the resulting distribution of stellar masses (§12.7).

The individual collapse of perturbed protostellar cores and their breakup into binaries and multiple systems have been studied extensively. Cores that match the density profiles of both starless and protostellar cores are found. The agreement is certainly remarkable. The density profiles of the majority of cores closely resemble that of the isothermal hydrostatic equilibrium solutions i.e. Bonnor-Ebert spheres. Nevertheless, the cores are far from equilibrium, being dynamically evolving. More evolved cores possess a $1/\mathrm{R}^2$ density profile, again consistent with the observations. The next step, yet to be achieved, is to model the velocity profiles of cores, to simulate observed turbulence and infall.

The accretion rates of widely-spread turbulent cores resemble quite closely that of triggered clouds. In a dense cluster environment, the accretion rates are high and highly variable. Since the collapse does not start from rest, very high accretion rates are achievable. High-mass stars tend to form early in the cluster evolution and then maintain high accretion rates. They may form in just a single free-fall time of $\sim 10^5$ years.

In contrast, low-mass stars tend to form later. After a high peak rate, the fall-off can take a wide variety of forms. Tidal interactions with other cores can cause a sudden halt to the accretion. On the other hand, merging of cores and competitive accretion of the available gas produce strong deviations from the smooth evolution of an isolated core. Finally, low-mass

cores may find themselves slung out of the cloud by dynamical instability, for example by the gravitational force during a close encounter with another core (see §5.5). Accretion may then terminate abruptly. The conclusion is that the accretion histories of protostellar cores can only be determined statistically.

8.7 Number, Age and Statistics

Class I sources are relatively rare compared to more exposed young stellar objects of Classes II and III found in and around molecular clouds. There are typically ten times less Class I than Class II. Assuming the class system corresponds to an evolutionary sequence, the relative number of sources in each evolutionary phase is proportional to the relative time spent in each phase. This statistical argument then suggests Class I ages in the range $1–5 \times 10^5$ years.

The Class 0 protostars are another factor of 10 less common than the Class I protostars in the ρ Ophiuchus cloud. This can be interpreted as a very abrupt babyhood for a star of $1–5 \times 10^4$ years. To accrete half of a solar mass in this time requires a mass accretion rate exceeding $10^{-5}\,\mathrm{M}_\odot\,\mathrm{yr}^{-1}$. Alternatively, the scarcity might be interpreted as a peculiarity of the star formation history in this particular region. Specifically, the rate of star formation may have quite sharply decreased about 2×10^5 years ago.

Class 0 sources are found in greater numbers in other locations. In the Taurus region, a region where star formation is more distributed, the duration of the Class 0 phase appears to be longer, $\sim 10^5$ years. Therefore, we should not think of protostars as isolated objects with evolutions determined solely by their initial conditions. More statistical data will help resolve these important issues.

We now also know that most pre-stellar cores must be young and evolve dynamically. Altogether, a good fraction (perhaps around one half) of all cores already harbour young stars. This was first shown in the 1980s by observations with IRAS, the Infrared Astronomical Satellite, which surveyed clouds for infrared sources, presumably a sign of strong accretion from an envelope. This indicates that pre-stellar cores are not long-lived equilibrium gas clouds but must also evolve fast: either collapsing or dispersing through fast dynamical processes rather than slow ambipolar diffusion.

There is further evidence that pre-stellar cores evolve dynamically. Smaller star formation regions contain stars with a narrower range in stellar

ages. The duration of star formation corresponds roughly to a few times the cloud crossing times at the turbulent speed. Furthermore, the spread in stellar ages in young clusters is small and comparable to the cluster dynamical time. In these situations, if starless cores could survive longer than $1\text{–}3 \times 10^6$ years, a range in stellar ages at least equal to this timespan would be predicted. Prime examples are from the Orion Trapezium cluster, the Taurus star formation region, and the NGC 1333 and NGC 6531 clusters.

8.8 Protostellar Evolution

How does the Class evolution occur? Whichever accretion model we choose, we face a problem in evolving a Class 0 source into a Class I source since it is not a transition in which mass is conserved. Instead, most of the core mass may be ejected.

First, it is essential to know how the central object is constructed. As noted above, this determines the radius of the protostar and, hence, the accretion luminosity. There are up to three stages we can tentatively identify for a low mass star. These are as follows:

- An initial growth phase to $0.3\,\mathrm{M}_\odot$, possibly with a constant radius.
- A linear growth in protostellar radius with accreted mass controlled by deuterium burning to $1\,\mathrm{M}_\odot$
- A small shrinkage as deuterium burning is suppressed, while accretion continues up to $3\,\mathrm{M}_\odot$.

A protostar will pass through all these stages only if sufficient mass is available. Higher mass stars will be considered later.

The first stage is rather uncertain. We could take a radius growing from zero to about $\sim$ 2–$3\,\mathrm{R}_\odot$ as the mass increases to $\sim 0.3\,\mathrm{M}_\odot$. If at constant average density, this would imply $M_* \propto R_*^3$, and, therefore, a rapidly increasing accretion luminosity but no luminosity due to contraction of the protostar itself.

The second stage is controlled by deuterium burning in the protostellar interior. While hydrogen burning does not commence until the star has reached the prime of its life, deuterium ignites when the central temperature reaches about 10^6 K. In a scenario where the protostar accretes at a constant rate of $10^{-5}\,\mathrm{M}_\odot\,\mathrm{yr}^{-1}$, this occurs when the protostar has reached a mass of just $0.3\,\mathrm{M}_\odot$. The energy input is then sufficient to generate and maintain convection. This means that newly-accreting material is caught up in the

convective eddies and rapidly transported to the centre. With constant accretion, we arrive at steady-state fuelling. The luminosity contributed by deuterium is then simply

$$L_D = \delta_D \dot{M} = 12 \left(\frac{\dot{M}}{10^{-5}\,\mathrm{M}_\odot\,\mathrm{yr}^{-1}} \right)\ \mathrm{L}_\odot, \tag{8.7}$$

where we assume a deuterium abundance of $[\mathrm{D/H}] = \delta_D = 2 \times 10^{-5}$ and δ_D is the nuclear energy released per unit mass.

The deuterium burning acts as a central thermostat, not allowing the temperature to rise above $\sim 10^6\,\mathrm{K}$ at this stage. In addition, the amount of available nuclear energy is comparable to the gravitational binding energy of the protostar, GM_*/R_*. This implies that the radius of the protostar will increase almost linearly with the mass. A detailed calculation shows that this leads to a $1\,\mathrm{M}_\odot$ protostar with a radius of $5\,\mathrm{R}_\odot$, if sufficient mass is available.

Thereafter, if the accretion continues, the protostar should become radiatively stable. That is, convection is not necessary. Rapid contraction follows until the protostar has accumulated a mass of about $3\,\mathrm{M}_\odot$. If this were to continue, hydrogen burning would soon commence, before the star had finished accreting. Instead, it is thought that deuterium re-ignites, this time in an outer convective shell, causing the protostar to swell up. This later evolution, however, is more relevant to the following chapter.

We can now estimate how the accretion luminosity evolves during a linear $M - R$ phase. Clearly, the luminosity is then directly proportional to the mass accretion rate,

$$L_{bol}(t) = 63 \left(\frac{\dot{M}}{10^{-5}\,\mathrm{M}_\odot\,\mathrm{yr}^{-1}} \right) \left(\frac{M_*}{1\mathrm{M}_\odot} \right) \left(\frac{R_*}{5\mathrm{R}_\odot} \right)^{-1}\ \mathrm{L}_\odot \tag{8.8}$$

and it exceeds L_D at all times, allowing us to equate the accretion power to the bolometric luminosity. In summary, the bolometric luminosity evolves quite closely with the mass accretion rate and can reach values of order 10–$100\,\mathrm{L}_\odot$.

It is remarkable that a star like the Sun reaches a much higher luminosity when young than it will obtain through nuclear burning on the main sequence. The total gravitational energy released in the collapse is given roughly by Eq. 4.7

$$-\mathcal{W} = 1.9 \times 10^7 \left(\frac{M}{M_\odot} \right)^2 \left(\frac{R}{R_\odot} \right)^{-1}\ \mathrm{L}_\odot \mathrm{yr}. \tag{8.9}$$

If this is released within an accretion phase lasting 1.9×10^5 yr, then the average luminosity is 100 times higher than from the present Sun.

Even more remarkable is that protostellar accretion offers us a great but fleeting opportunity to detect lower mass objects. Even brown dwarfs can produce a high luminosity during their formation. This is important because stars on the main sequence generate nuclear power at a rate $L_{nuc} \propto M^4$. This implies that low-mass stars evolve very slowly but are difficult to find. In contrast, according to Eq. 8.8, although there is less of it, gravitational energy is released at a much higher rate. Therefore, the formation stage is the best possibility we have at present to investigate very low-mass stars.

8.9 Protostellar Envelopes

The events described above are obscured. We cannot directly see a protostar's photosphere because the emitted radiation is absorbed by the dust in the surrounding envelope. The warmed dust then radiates at longer wavelengths. This process may be repeated until the radiation reaches a wavelength which the dust no longer intercepts. From the observer's view, the depth that we can penetrate from the outside into the dust determines a dust photospheric size. The dust photospheric radius depends on the amount of dust and the opacity, which itself depends on the wavelength.

Between the protostar's photosphere and the dust envelope lies an *opacity gap* across which the radiation propagates unhindered. The dust in this region has been evaporated provided the temperature exceeds $\sim$ 1,500 K. The region is also expected to become progressively vacated as more material falls onto the accretion disk and less heads directly towards the protostar.

The actual physical outer edge to the envelope may lie far beyond the dust photosphere. We define this edge in terms of the core temperature: when the temperature of the core has dropped to that of the ambient cloud, the core is no longer distinguishable. To determine the total mass in the envelope, which is probably the mass reservoir from which a star can be constructed, we need to take a sufficiently long wavelength so that all the dust emission is able to escape from within the photosphere, in addition to the dust outside. Millimetre wavelength observations may thus determine the total dust mass which has been warmed by the protostar, both inside and outside the dust photosphere. This dust mass can be converted to a

gas mass, on applying some quite well-tested correlations between the two.

The simplest approach is to model the envelope with power-law radial distributions for the density and temperature. However, there remain tremendous uncertainties in the derived results.

To proceed further, we need to model the parts we usually can't see. An accretion disk should be hidden within the envelope, mediating the flow from the envelope to the protostar. We define an inner edge to the envelope as where angular momentum provides a centrifugal barrier, turning spherical accretion into disk accretion. The envelope loses mass as the system evolves; first to the protostar, then to the disk and then through dispersal. At some stage the envelope becomes optically thin and the disk and protostar will be exposed.

In order to match the observations, we model the mass infall from the envelope as follows. After a sharp initial rise, a peak accretion rate is reached to reproduce the Class 0 stage. This mass passes through the disk, accumulating onto the protostar's surface. As the envelope mass is reduced, the accretion rate from it also falls. This has the effect of reducing the size of the dust photosphere, which tends to increase the bolometric temperature. It also increases the mass of the star relative to the envelope.

These changes should automatically produce a Class I protostar. However, we find that too much mass remains in the envelope, even though the central protostar has accumulated most of its final mass. To make the evolution work, we need the envelope to lose most of its mass in other ways, not to the protostar. How this is achieved remains a mystery although there are processes which could accomplish the deed: disruptive interactions with the environment and dispersing winds driven by protostellar jets.

8.10 Summary: Observation versus Theory

The rates of mass accretion of Class 0 sources are believed to be higher than those of Class I souces. One important line of circumstantial evidence is derived from the CO outflow activity. As noted above, Class 0 sources have an order of magnitude larger power and momentum flux in their outflows than those of Class I sources. Most ejection models predict that the momentum flux of the outflow is proportional to the accretion rate. This implies that these Class 0 sources experience higher accretion rates.

Secondly, and more directly, radiative transfer calculations of infalling, dusty envelopes surrounding Class 0 protostars yield accretion rates ex-

ceeding 10^{-4} $M_\odot$ yr^{-1}. Both modelling of the far-infrared peaks in the SED and molecular line modelling support high mass accretion rates. This rate is much higher than the typical accretion rates of $\sim 3 \times 10^{-6}$ $M_\odot$ yr^{-1} of the Class I sources (in Taurus-Auriga), whose values were obtained by similar radiative transfer calculations.

In terms of initially static models, the high accretion rates of Class 0 sources may be explained by beginning from an appropriate density profile. Before collapse begins, a flat inner region surrounded by a power-law envelope is required. In terms of dynamical models, numerical simulations display abrupt collapse and accretion onto dense filaments and cores.

All the isothermal 'similarity' solutions share a universal evolutionary pattern. At early times, a compression wave (initiated by, e.g., an external disturbance) propagates inward at the sound speed, leaving behind it a $\rho(R) \propto R^{-2}$ density profile. At t = 0, the compression wave reaches the centre and a point mass forms which subsequently grows by accretion. At later times, this wave is reflected into a rarefaction or expansion wave, propagating outward (also at the sound speed) through the infalling gas, and leaving behind it a free-fall zone with a $\rho(R) \propto R^{-1.5}$ density distribution.

As already noted above, a problem for the inside-out collapse scenario is the detection of extended zones of infall in cores which have still to develop a recognisable protostellar nucleus. The observed infall asymmetry is spatially too extended (0.1 pc) to be consistent with this collapse model. A related problem is that collapse should set in well before the $\rho \propto 1/R^2$ profile is achieved. The collapse will, however, be mediated by the magnetic field and angular momentum. So this cannot be the complete picture and a modified version of the above scenario could still prove viable.